Journal of Modern Optics
Vol. 57, No. 19, 10 November 2010, 1908–1915

Quantum properties of a spatially-broadband traveling-wave phase-sensitive optical parametric amplifier

Michael Vasilyev[a], Muthiah Annamalai[a], Nikolai Stelmakh[a]* and Prem Kumar[b]

[a]*Department of Electrical Engineering, University of Texas at Arlington, 416 Yates St., Arlington, TX 76019, USA;* [b]*Center for Photonic Communication and Computing, EECS Department, Northwestern University, 2145 Sheridan Rd., Evanston, IL 60208, USA*

(*Received 26 March 2010; final version received 17 May 2010*)

We present the quantum theory of a spatially-multimode traveling-wave phase-sensitive optical parametric amplifier (OPA) pumped by a beam with arbitrary spatial profile. By using Green's functions of the classical OPA, we derive the normally-ordered quadrature correlators at the OPA output, which provide complete quantum description of the phase-sensitive OPA and enable determination of its independently-squeezed eigenmodes. Two analytically treatable examples of plane-wave pump and infinite spatial bandwidth of the crystal are discussed in detail.

Keywords: optical parametric amplifiers; phase-sensitive amplifiers; image amplification; quantum noise squeezing

1. Introduction

Spatially-broadband optical parametric amplifiers (OPAs) are important for the generation of correlated modes for quantum information processing as well as for noiseless amplification of images, with recent work nicely summarized in [1,2]. The latter application requires phase-sensitive OPAs with strongly focused pump beams in either traveling-wave [3,4] or self-imaging-cavity [5] configurations. While the classical traveling-wave OPA with plane-wave pump has a well known analytical solution [6,7] that is straightforwardly extendable to the quantum case, the inhomogeneous (i.e. spatially-varying) pump case requires numerical modeling even for the classical signal [8], unless the nonlinear medium of the OPA is very short. Although computationally efficient numerical methods based on Hermite–Gaussian and Laguerre–Gaussian mode expansions have been developed for both cavity-based [9] and traveling-wave [10] OPAs for some pumping configurations, determination of the complete quantum properties of the OPAs from numerical modeling have remained a serious challenge.

In this work, we provide a general framework relating the complete quantum description of the traveling-wave phase-sensitive OPA with arbitrary pump to Green's function of the underlying classical propagation equation, which is obtainable by numerical or (in rare instances) analytical methods. By diagonalizing the derived quantum correlators, we show that a set of independently-squeezed orthogonal modes (eigenmodes) of the OPA can be obtained, in analogy to the Karhunen–Loève expansion for classical random processes. Such eigenmodes of the traveling-wave OPA are also related to the supermodes of a self-imaging-cavity-based OPA studied in [11]. The analysis of the present paper serves as a basis for our determination of the actual OPA eigenmodes via numerically-obtained Green's functions in Hermite–Gaussian representation [12].

2. Definitions from classical free-space propagation

A detailed theory of parametric amplification of multimode fields is summarized in a recently published book [1]. Here, we concentrate on OPA equations in paraxial approximation with undepleted pump. Assuming that the signal, idler, and pump fields are polarized, we look for solutions in the form

$$e(\vec{r}, t) = E(\vec{\rho}, z)e^{i(kz-\omega t)} + c.c., \tag{1}$$

where $E(\vec{\rho}, z)$ is a slowly-varying field envelope, $\vec{\rho}$ is a transverse vector with coordinates (x, y), and the intensity is given by

$$I(\vec{\rho}, z) = 2\varepsilon_0 nc|E(\vec{\rho}, z)|^2. \tag{2}$$

*Corresponding author. Email: nikolais@uta.edu

ISSN 0950–0340 print/ISSN 1362–3044 online

DOI: 10.1080/09500340.2010.495463
http://www.informaworld.com

In the presence of a strong pump $E_p(\vec{\rho}, z)$ at frequency ω_p, signal electric field $E_s(\vec{\rho}, z)$ at frequency ω_s is coupled to the idler electric field $E_i(\vec{\rho}, z)$ at frequency $\omega_i = \omega_p - \omega_s$ through the following equation:

$$\frac{\partial E_s}{\partial z} = \frac{i}{2k_s}\nabla_\rho^2 E_s + \frac{i\omega_s d_{\text{eff}}}{n_s c} E_p E_i^* e^{i\Delta k z}, \tag{3}$$

where $\Delta k = k_p - k_s - k_i$ is the wavevector mismatch, d_{eff} is the effective nonlinear coefficient accounting for the field polarizations and crystal orientation, and the equation for the idler beam is obtained by interchanging subscripts s and i in Equation (3). Equation (3) describes the traveling-wave OPA in paraxial approximation with a pump of arbitrary spatial profile.

Let us introduce the spatial-frequency ($\vec{q}$) domain through the Fourier transform

$$\tilde{E}(\vec{q}, z) = \int E(\vec{\rho}, z) e^{-i\vec{q}\vec{\rho}} \mathrm{d}\vec{\rho} \tag{4}$$

and the inverse Fourier transform

$$E(\vec{\rho}, z) = \int \tilde{E}(\vec{q}, z) e^{i\vec{q}\vec{\rho}} \frac{\mathrm{d}\vec{q}}{(2\pi)^2}. \tag{5}$$

In the absence of the pump ($E_p = 0$), Equation (3) is reduced to the paraxial Helmholtz equation, whose solution in the Fourier domain is given by

$$\tilde{E}(\vec{q}, z) = \tilde{E}(\vec{q}, 0)\exp\left(-i\frac{q^2}{2k}z\right), \tag{6}$$

which translates into the following spatial-domain solutions (Fresnel integrals):

$$E(\vec{\rho}, z) = \frac{k}{2\pi i z}\int E(\vec{\rho}\,', 0)\exp\left[\frac{ik|\vec{\rho} - \vec{\rho}\,'|^2}{2z}\right]\mathrm{d}\vec{\rho}\,', \quad \text{(2D)} \tag{7}$$

$$E(x, z) = \sqrt{\frac{k}{2\pi z}} e^{-i\pi/4}\int E(x', 0)\exp\left[\frac{ik(x - x')^2}{2z}\right]\mathrm{d}x', \quad \text{(1D)} \tag{8}$$

where the kernels of integrals in Equations (7) and (8) are, respectively, the 2D and 1D Green's functions

$$G(\vec{\rho}, \vec{\rho}\,', z) = \frac{k}{2\pi i z}\exp\left[i\frac{k|\vec{\rho} - \vec{\rho}\,'|^2}{2z}\right], \quad \text{(2D)} \tag{9}$$

$$G(x, x', z) = \sqrt{\frac{k}{2\pi z}} e^{-i\pi/4}\exp\left[i\frac{k(x - x')^2}{2z}\right], \quad \text{(1D)} \tag{10}$$

i.e. the solutions of the paraxial Helmholtz equation satisfying the initial conditions

$$G(\vec{\rho}, \vec{\rho}\,', 0) = \delta(\vec{\rho} - \vec{\rho}\,'), \quad \text{(2D)} \tag{11}$$

$$G(x, x', 0) = \delta(x - x'). \quad \text{(1D)} \tag{12}$$

3. Degenerate OPA

Assuming the signal and idler beam to have the same frequency and polarization, we can drop the s and i subscripts. We can express the signal field in terms of two real-valued quadratures,

$$E(\vec{\rho}, z) = X(\vec{\rho}, z) + iY(\vec{\rho}, z), \tag{13}$$

so that the solution is given by

$$E(\vec{\rho}, z) = \int [G_x(\vec{\rho}, \vec{\rho}\,', z)X(\vec{\rho}\,', 0) + iG_y(\vec{\rho}, \vec{\rho}\,', z)Y(\vec{\rho}\,', 0)]\mathrm{d}\vec{\rho}\,', \tag{14}$$

where $G_x(\vec{\rho}, \vec{\rho}\,', z)$ and $iG_y(\vec{\rho}, \vec{\rho}\,', z)$ are the Green's functions of Equation (3), i.e. its solutions with initial conditions

$$\begin{aligned} G_x(\vec{\rho}, \vec{\rho}\,', 0) &= \delta(\vec{\rho} - \vec{\rho}\,'), \\ iG_y(\vec{\rho}, \vec{\rho}\,', 0) &= i\delta(\vec{\rho} - \vec{\rho}\,'). \end{aligned} \tag{15}$$

The solution (14) can be re-written in vector form as

$$\mathbf{E}(\vec{\rho}, z) = \int \mathbf{G}(\vec{\rho}, \vec{\rho}\,', z)\mathbf{E}(\vec{\rho}\,', 0)\,\mathrm{d}\vec{\rho}\,', \tag{16}$$

where

$$\mathbf{E}(\vec{\rho}, z) = \begin{bmatrix} X(\vec{\rho}, z) \\ Y(\vec{\rho}, z) \end{bmatrix}, \tag{17}$$

$$\mathbf{G}(\vec{\rho}, \vec{\rho}\,', z) = \begin{bmatrix} C_x(\vec{\rho}, \vec{\rho}\,', z) & C_y(\vec{\rho}, \vec{\rho}\,', z) \\ S_x(\vec{\rho}, \vec{\rho}\,', z) & S_y(\vec{\rho}, \vec{\rho}\,', z) \end{bmatrix}, \tag{18}$$

and the elements of real matrix $\mathbf{G}$ in Equation (18) are related to G_x and G_y of Equation (14) as follows:

$$\begin{aligned} G_x(\vec{\rho}, \vec{\rho}\,', z) &= C_x(\vec{\rho}, \vec{\rho}\,', z) + iS_x(\vec{\rho}, \vec{\rho}\,', z), \\ G_y(\vec{\rho}, \vec{\rho}\,', z) &= S_y(\vec{\rho}, \vec{\rho}\,', z) - iC_y(\vec{\rho}, \vec{\rho}\,', z). \end{aligned} \tag{19}$$

Note that Equation (16) can also be written in the spatial-frequency domain as

$$\tilde{\mathbf{E}}(\vec{q}, z) = \int \tilde{\mathbf{G}}(\vec{q}, -\vec{q}\,', z)\tilde{\mathbf{E}}(\vec{q}\,', 0)\frac{\mathrm{d}\vec{q}\,'}{(2\pi)^2}, \tag{20}$$

where

$$\tilde{\mathbf{E}}(\vec{q}, z) = \begin{bmatrix} \tilde{X}(\vec{q}, z) \\ \tilde{Y}(\vec{q}, z) \end{bmatrix} = \begin{bmatrix} \frac{\tilde{E}(\vec{q}, z) + \tilde{E}^*(-\vec{q}, z)}{2} \\ \frac{\tilde{E}(\vec{q}, z) - \tilde{E}^*(-\vec{q}, z)}{2i} \end{bmatrix} \tag{21}$$

is the Fourier transform of electric field in equation (17), and $\tilde{\mathbf{G}}(\vec{q},\vec{q}\,',z)$ is the Fourier transform of the Green's function (18) with respect to both $\vec{\rho}$ and $\vec{\rho}\,'$.

3.1. Quantum description of the degenerate OPA

Since Equation (3) is linear, it (as well as all the other formulae above) also holds in the quantum case by assuming the signal electric field to be an operator. It is convenient to normalize this operator so as to produce the following commutation relations:

$$\begin{aligned}[E(\vec{\rho},z),E^{+}(\vec{\rho}\,',z)]&=\delta(\vec{\rho}-\vec{\rho}\,'),\\ [E(\vec{\rho},z),E(\vec{\rho}\,',z)]&=0.\end{aligned}\tag{22}$$

Preservation of the commutators (22) during the field evolution in the OPA requires that

$$\begin{aligned}&\int[C_x(\vec{\rho},\vec{\rho}\,'',z)C_y(\vec{\rho}\,',\vec{\rho}\,'',z)-C_y(\vec{\rho},\vec{\rho}\,'',z)C_x(\vec{\rho}\,',\vec{\rho}\,'',z)]\,\mathrm{d}\vec{\rho}\,''=0,\\ &\int[S_x(\vec{\rho},\vec{\rho}\,'',z)S_y(\vec{\rho}\,',\vec{\rho}\,'',z)-S_y(\vec{\rho},\vec{\rho}\,'',z)S_x(\vec{\rho}\,',\vec{\rho}\,'',z)]\,\mathrm{d}\vec{\rho}\,''=0,\\ &\int[C_x(\vec{\rho},\vec{\rho}\,'',z)S_y(\vec{\rho}\,',\vec{\rho}\,'',z)-C_y(\vec{\rho},\vec{\rho}\,'',z)S_x(\vec{\rho}\,',\vec{\rho}\,'',z)]\,\mathrm{d}\vec{\rho}\,''\\ &\quad=\delta(\vec{\rho}-\vec{\rho}\,'),\\ &\int[S_y(\vec{\rho},\vec{\rho}\,'',z)C_x(\vec{\rho}\,',\vec{\rho}\,'',z)-S_x(\vec{\rho},\vec{\rho}\,'',z)C_y(\vec{\rho}\,',\vec{\rho}\,'',z)]\,\mathrm{d}\vec{\rho}\,''\\ &\quad=\delta(\vec{\rho}-\vec{\rho}\,'),\end{aligned}\tag{23}$$

which can be expressed in the matrix form as

$$\int\mathbf{G}(\vec{\rho},\vec{\rho}\,'',z)\mathbf{J}^{\mathrm{T}}\mathbf{G}^{\mathrm{T}}(\vec{\rho}\,',\vec{\rho}\,'',z)\mathbf{J}\,\mathrm{d}\vec{\rho}\,''=\begin{bmatrix}\delta(\vec{\rho}-\vec{\rho}\,') & 0\\ 0 & \delta(\vec{\rho}-\vec{\rho}\,')\end{bmatrix},\tag{24}$$

where

$$\mathbf{J}^{\mathrm{T}}\mathbf{G}^{\mathrm{T}}(\vec{\rho},\vec{\rho}\,',z)\mathbf{J}=\begin{bmatrix}S_y(\vec{\rho},\vec{\rho}\,',z) & -C_y(\vec{\rho},\vec{\rho}\,',z)\\ -S_x(\vec{\rho},\vec{\rho}\,',z) & C_x(\vec{\rho},\vec{\rho}\,',z)\end{bmatrix}.\tag{25}$$

Equation (24) means that the transformation in Equation (16) is symplectic, i.e. it preserves an antisymmetric matrix

$$\mathbf{J}=\begin{bmatrix}0 & 1\\ -1 & 0\end{bmatrix}.\tag{26}$$

Assuming the state at the input of the OPA to be vacuum (coherent state is treated the same way by separating the classical mean field from the vacuum fluctuations), we can completely describe the quantum properties of the output light by a correlation matrix

$$\mathbf{R}(\vec{\rho},\vec{\rho}\,',z)=4\times\begin{bmatrix}\langle X(\vec{\rho},z)X(\vec{\rho}\,',z)\rangle & \langle X(\vec{\rho},z)Y(\vec{\rho}\,',z)\rangle\\ \langle Y(\vec{\rho},z)X(\vec{\rho}\,',z)\rangle & \langle Y(\vec{\rho},z)Y(\vec{\rho}\,',z)\rangle\end{bmatrix},\tag{27}$$

whose value at the OPA input is

$$\mathbf{R}(\vec{\rho},\vec{\rho}\,',0)=\delta(\vec{\rho}-\vec{\rho}\,')\times\begin{bmatrix}1 & i\\ -i & 1\end{bmatrix}.\tag{28}$$

The elements of the correlation matrix in Equation (27), to be referred to as the correlators, are given by

$$\begin{aligned}\langle X(\vec{\rho},z)X(\vec{\rho}\,',z)\rangle&=\frac{1}{4}\int[C_x(\vec{\rho},\vec{\rho}\,'',z)C_x(\vec{\rho}\,',\vec{\rho}\,'',z),\\ &\quad+C_y(\vec{\rho},\vec{\rho}\,'',z)C_y(\vec{\rho}\,',\vec{\rho}\,'',z)]\,\mathrm{d}\vec{\rho}\,''\\ \langle Y(\vec{\rho},z)Y(\vec{\rho}\,',z)\rangle&=\frac{1}{4}\int[S_x(\vec{\rho},\vec{\rho}\,'',z)S_x(\vec{\rho}\,',\vec{\rho}\,'',z)\\ &\quad+S_y(\vec{\rho},\vec{\rho}\,'',z)S_y(\vec{\rho}\,',\vec{\rho}\,'',z)]\,\mathrm{d}\vec{\rho}\,'',\\ \langle X(\vec{\rho},z)Y(\vec{\rho}\,',z)\rangle&=\frac{i}{4}\delta(\vec{\rho}-\vec{\rho}\,')+\langle X(\vec{\rho},z)Y(\vec{\rho}\,',z)\rangle_N,\\ \langle Y(\vec{\rho},z)X(\vec{\rho}\,',z)\rangle&=-\frac{i}{4}\delta(\vec{\rho}-\vec{\rho}\,')+\langle Y(\vec{\rho},z)X(\vec{\rho}\,',z)\rangle_N,\\ \langle X(\vec{\rho},z)Y(\vec{\rho}\,',z)\rangle_N&=\frac{1}{4}\int[C_x(\vec{\rho},\vec{\rho}\,'',z)S_x(\vec{\rho}\,',\vec{\rho}\,'',z)\\ &\quad+C_y(\vec{\rho},\vec{\rho}\,'',z)S_y(\vec{\rho}\,',\vec{\rho}\,'',z)]\,\mathrm{d}\vec{\rho}\,'',\\ \langle Y(\vec{\rho},z)X(\vec{\rho}\,',z)\rangle_N&=\frac{1}{4}\int[S_x(\vec{\rho},\vec{\rho}\,'',z)C_x(\vec{\rho}\,',\vec{\rho}\,'',z)\\ &\quad+S_y(\vec{\rho},\vec{\rho}\,'',z)C_y(\vec{\rho}\,',\vec{\rho}\,'',z)]\,\mathrm{d}\vec{\rho}\,'',\end{aligned}\tag{29}$$

where the subscript N denotes a normally-ordered correlator. Eliminating the delta-function from the off-diagonal elements of Equation (27) yields a related correlation matrix

$$\mathbf{R}'(\vec{\rho},\vec{\rho}\,',z)=4\times\begin{bmatrix}\langle X(\vec{\rho},z)X(\vec{\rho}\,',z)\rangle & \langle X(\vec{\rho},z)Y(\vec{\rho}\,',z)\rangle_N\\ \langle Y(\vec{\rho},z)X(\vec{\rho}\,',z)\rangle_N & \langle Y(\vec{\rho},z)Y(\vec{\rho}\,',z)\rangle\end{bmatrix}\tag{30}$$

with initial conditions

$$\mathbf{R}'(\vec{\rho},\vec{\rho}\,',0)=\delta(\vec{\rho}-\vec{\rho}\,')\times\begin{bmatrix}1 & 0\\ 0 & 1\end{bmatrix}.\tag{31}$$

One can also see that $\mathbf{R}'(\vec{\rho},\vec{\rho}\,',z)=\mathbf{R}'(\vec{\rho},\vec{\rho}\,',0)+\mathbf{R}'_N(\vec{\rho},\vec{\rho}\,',z)$, where $\mathbf{R}'_N(\vec{\rho},\vec{\rho}\,',z)$ has zero initial condition and is given by Equation (30) with the diagonal-element correlators replaced by the corresponding normally-ordered correlators. It is easy to show that

$$\mathbf{R}'(\vec{\rho},\vec{\rho}\,',z)=\int\mathbf{G}(\vec{\rho},\vec{\rho}\,'',z)\mathbf{G}^{\mathrm{T}}(\vec{\rho}\,',\vec{\rho}\,'',z)\,\mathrm{d}\vec{\rho}\,''.\tag{32}$$

In the spatial-frequency domain, this correlation matrix is given by

$$\begin{aligned}\tilde{\mathbf{R}}'(\vec{q},\vec{q}\,',z)&=\int\mathbf{R}'(\vec{\rho},\vec{\rho}\,',z)e^{-i\vec{q}\vec{\rho}}e^{-i\vec{q}\,'\vec{\rho}\,'}\,\mathrm{d}\vec{\rho}\,\mathrm{d}\vec{\rho}\,'\\ &=\int\tilde{\mathbf{G}}(\vec{q},\vec{q}\,'',z)\tilde{\mathbf{G}}^{\mathrm{T}}(\vec{q}\,',-\vec{q}\,'',z)\frac{\mathrm{d}\vec{q}\,''}{(2\pi)^2}.\end{aligned}\tag{33}$$

The Green's functions in Equation (14) can, in general, be found numerically (analytical solutions are known for the case of a plane-wave pump and the case of a very short crystal with inhomogeneous pump), which enables the evaluation of the correlators in Equations (27), (29), (30), (32), and (33).

3.2. Modes of maximum squeezing and anti-squeezing

Let us project the amplified light onto a mode

$$\mathbf{E}_{\mathrm{LO}} = \begin{bmatrix} X_{\mathrm{LO}}(\vec{\rho}) \\ Y_{\mathrm{LO}}(\vec{\rho}) \end{bmatrix}, \tag{34}$$

called the local oscillator (LO) mode. The detected squeezing factor (measured noise normalized by the standard quantum limit) is given by

$$\lambda(z) = \frac{\iint \mathbf{E}^{\mathbf{T}}_{\mathbf{LO}}(\vec{\rho})\mathbf{R}(\vec{\rho},\vec{\rho}',z)\mathbf{E}_{\mathbf{LO}}(\vec{\rho}')\,\mathrm{d}\vec{\rho}\mathrm{d}\vec{\rho}'}{\int \mathbf{E}^{\mathbf{T}}_{\mathbf{LO}}(\vec{\rho})\mathbf{E}_{\mathbf{LO}}(\vec{\rho})\,\mathrm{d}\vec{\rho}}, \tag{35}$$

where the kernel $\mathbf{R}(\vec{\rho},\vec{\rho}',z)$ obtained from Equation (27) is Hermitian, i.e.

$$\mathbf{R}^{+}(\vec{\rho},\vec{\rho}',z) = \mathbf{R}(\vec{\rho}',\vec{\rho},z). \tag{36}$$

Equation (35) would still hold if we replace the kernel $\mathbf{R}(\vec{\rho},\vec{\rho}',z)$ by $\mathbf{R}'(\vec{\rho},\vec{\rho}',z)$, which is also Hermitian, but is more convenient for numerical evaluations. The projection (35) onto the LO mode can also be done in the spatial-frequency domain:

$$\lambda(z) = \frac{\iint \tilde{\mathbf{E}}^{\mathbf{T}}_{\mathbf{LO}}(\vec{q})\tilde{\mathbf{R}}'^{*}(\vec{q},\vec{q}',z)\tilde{\mathbf{E}}_{\mathbf{LO}}(\vec{q}')\frac{\mathrm{d}\vec{q}\mathrm{d}\vec{q}'}{(2\pi)^4}}{\int \tilde{\mathbf{E}}^{\mathbf{T}}_{\mathbf{LO}}(\vec{q})\tilde{\mathbf{E}}^{*}_{\mathbf{LO}}(\vec{q})\frac{\mathrm{d}\vec{q}}{(2\pi)^2}}, \tag{37}$$

where

$$\tilde{\mathbf{E}}^{*}_{\mathbf{LO}}(\vec{q}) = \tilde{\mathbf{E}}_{\mathbf{LO}}(-\vec{q}) \tag{38}$$

and

$$\tilde{\mathbf{R}}'^{*}(\vec{q},\vec{q}',z) = \tilde{\mathbf{R}}'(-\vec{q},\,-\vec{q}',z). \tag{39}$$

Once we obtain the correlation matrix $\mathbf{R}(\vec{\rho},\vec{\rho}',z)$ or $\mathbf{R}'(\vec{\rho},\vec{\rho}',z)$ from the Green's functions, we can find the extrema of the functional (35) (known as the Rayleigh quotient) as eigensolutions of the Fredholm integral equation

$$\int \mathbf{R}'(\vec{\rho},\vec{\rho}',z)\mathbf{E}^{\lambda}_{\mathrm{LO}}(\vec{\rho}')\,\mathrm{d}\vec{\rho}' = \lambda(z)\mathbf{E}^{\lambda}_{\mathbf{LO}}(\vec{\rho}), \tag{40}$$

which defines a complete set of orthogonal uncorrelated modes $\mathbf{E}^{\lambda}_{\mathbf{LO}}(\vec{\rho})$, classified by their squeezing factors λ. This procedure is a quantum analog of the standard Karhunen–Loève expansion. If

$$\mathbf{E}^{\lambda}_{\mathbf{LO}}(\vec{\rho}) = \begin{bmatrix} X_{\mathrm{LO}}(\vec{\rho}) \\ Y_{\mathrm{LO}}(\vec{\rho}) \end{bmatrix} \tag{41}$$

is an eigenmode of Equation (40) with eigenvalue $\lambda < 1$ (squeezed quadrature), then

$$\mathbf{E}^{1/\lambda}_{\mathbf{LO}}(\vec{\rho}) = \mathbf{J}\,\mathbf{E}^{\lambda}_{\mathbf{LO}}(\vec{\rho}) = \begin{bmatrix} Y_{\mathrm{LO}}(\vec{\rho}) \\ -X_{\mathrm{LO}}(\vec{\rho}) \end{bmatrix} \tag{42}$$

is also an eigenmode of Equation (40) with eigenvalue $1/\lambda > 1$ (anti-squeezed quadrature). The mode $\mathbf{E}^{1/\lambda}_{\mathbf{LO}}(\vec{\rho})$ is a $-\pi/2$-shifted version of $\mathbf{E}^{\lambda}_{\mathbf{LO}}(\vec{\rho})$. Note that in the spatial-frequency domain, Equation (40) takes the form

$$\int \tilde{\mathbf{R}}'(\vec{q},\,-\vec{q}',z)\tilde{\mathbf{E}}^{\lambda}_{\mathbf{LO}}(\vec{q}')\frac{\mathrm{d}\vec{q}'}{(2\pi)^2} = \lambda(z)\tilde{\mathbf{E}}^{\lambda}_{\mathbf{LO}}(\vec{q}). \tag{43}$$

Thus, by solving Equation (40) one can obtain the shapes of the independently-squeezed modes, and their spectrum of squeezing/anti-squeezing, for an arbitrary pump profile. This will completely answer the questions about the effective number of amplified modes and their spatial profiles. Possibilities for additional analysis include (a) iteration of the pump profile to maximize the number of well-squeezed modes (i.e. spatial 'bandwidth' of squeezing) and (b) finding a unitary transformation that maps these modes to known modes, e.g. Hermite–Gaussian modes or plane waves (in the latter case, λ becomes the spatial squeezing spectrum).

It is worth noting that the procedure for diagonalizing the case of multimode squeezing into independently-squeezed modes was originally developed in a general form in [13,14] for the case an arbitrary quadratic Hamiltonian. The theory for optimal (matched) LO with Equations (35) and (40) was introduced in [15] and later applied to the calculation of soliton squeezing in [16,17]. Similar decomposition techniques were recently reviewed in [18] in the context of parametric interactions in optical fibers.

3.3. Analytical solution 1: plane-wave pump

In the presence of a plane-wave pump $E_p(\vec{\rho},z) = |E_p|e^{i\theta_p} = const$, Equation (3) still preserves the shift-invariance of the original paraxial Helmholtz equation and is, therefore, easily solved in the Fourier domain [6]:

$$\tilde{E}_s(\vec{q},z) = \mu(q,z)\tilde{E}_s(\vec{q},0) + \nu(q,z)\tilde{E}^{*}_{i}(-\vec{q},0), \tag{44}$$

where the coefficients of the input–output transformation are

$$\mu(q,z) = \left(\cosh\gamma z - \frac{i\Delta k_{\mathrm{eff}}}{2\gamma}\sinh\gamma z\right) \times \exp\left(i\frac{\Delta k_{\mathrm{eff}}}{2}z\right)\exp\left(-i\frac{q^2}{2k_s}z\right),$$
$$\nu(q,z) = i\frac{\kappa_s}{\gamma}\sinh\gamma z \times \exp\left(i\frac{\Delta k_{\mathrm{eff}}}{2}z\right)\exp\left(-i\frac{q^2}{2k_s}z\right), \tag{45}$$

$q = |\vec{q}|$, the effective wavevector mismatch is

$$\begin{aligned}\Delta k_{\text{eff}} &= k_p - k_s - k_i + \frac{q^2}{2}\left(\frac{1}{k_s} + \frac{1}{k_i}\right) \\ &= \Delta k + \frac{q^2}{2}\left(\frac{1}{k_s} + \frac{1}{k_i}\right),\end{aligned} \tag{46}$$

and the parametric gain coefficient is

$$\gamma = \sqrt{\kappa^2 - \Delta k_{\text{eff}}^2/4}, \tag{47}$$

with

$$\kappa^2 = \kappa_s \kappa_i^* = \frac{\omega_s \omega_i d_{\text{eff}}^2 I_p}{2\varepsilon_0 n_s n_i n_p c^3},$$

$$\kappa_s = \frac{\omega_s d_{eff}}{n_s c} |E_p| e^{i\theta_p}.$$

Note that, in the degenerate case, the product of the exponentials in Equation (45), containing the effective wavevector mismatch and diffraction phase terms, becomes simply $\exp(i\Delta kz/2)$.

From this point on, we will assume wavelength- and polarization-degenerate signal and idler waves, which allows us to drop the s and i subscripts. Green's functions in the plane-wave pump case are given by

$$\begin{aligned}G_x(\vec{\rho}, \vec{\rho}\,', z) &= \int e^{i\vec{q}(\vec{\rho}-\vec{\rho}\,')}[\mu(q,z) + \nu(q,z)]\frac{\mathrm{d}\vec{q}}{(2\pi)^2} \\ &= G_x(|\vec{\rho} - \vec{\rho}\,'|, z), \\ G_y(\vec{\rho}, \vec{\rho}\,', z) &= \int e^{i\vec{q}(\vec{\rho}-\vec{\rho}\,')}[\mu(q,z) - \nu(q,z)]\frac{\mathrm{d}\vec{q}}{(2\pi)^2} \\ &= G_y(|\vec{\rho} - \vec{\rho}\,'|, z),\end{aligned} \tag{48}$$

where the μ and ν coefficients are taken from Equation (45). In the spatial-frequency domain, the matrix form of Green's function is given by

$$\tilde{\mathbf{G}}(\vec{q}, \vec{q}\,', z) = (2\pi)^2 \delta(\vec{q} + \vec{q}\,')\mathbf{M}(q, z), \tag{49}$$

where

$$\mathbf{M}(q,z) = \begin{bmatrix} \mathrm{Re}(\mu+\nu) & -\mathrm{Im}(\mu-\nu) \\ \mathrm{Im}(\mu+\nu) & \mathrm{Re}(\mu-\nu) \end{bmatrix}, \tag{50}$$

that is

$$\tilde{\mathbf{E}}(\vec{q}, z) = \mathbf{M}(q, z)\tilde{\mathbf{E}}(\vec{q}, 0). \tag{51}$$

The correlation-matrix kernel $\tilde{\mathbf{R}}'(\vec{q}, \vec{q}\,', z)$ is, therefore, given by

$$\begin{aligned}\tilde{\mathbf{R}}'(\vec{q}, \vec{q}\,', z) &= (2\pi)^2 \delta(\vec{q} + \vec{q}\,')\mathbf{M}(q,z)\mathbf{M}^{\mathbf{T}}(q,z) \\ &= (2\pi)^2 \delta(\vec{q} + \vec{q}\,')\begin{bmatrix} |\mu + \nu^*|^2 & 2\mathrm{Im}(\mu\nu) \\ 2\mathrm{Im}(\mu\nu) & |\mu - \nu^*|^2 \end{bmatrix},\end{aligned} \tag{52}$$

the squeezing/anti-squeezing factor is determined by

$$\lambda(z) = \frac{\int \tilde{\mathbf{E}}_{\mathbf{LO}}^{\mathbf{T}}(\vec{q})\mathbf{M}(q,z)\mathbf{M}^{\mathbf{T}}(q,z)\tilde{\mathbf{E}}_{\mathbf{LO}}^*(\vec{q})\frac{\mathrm{d}\vec{q}}{(2\pi)^2}}{\int \tilde{\mathbf{E}}_{\mathbf{LO}}^{\mathbf{T}}(\vec{q})\tilde{\mathbf{E}}_{\mathbf{LO}}^*(\vec{q})\frac{\mathrm{d}\vec{q}}{(2\pi)^2}}, \tag{53}$$

and the independently squeezed modes are the eigenvectors of the matrix $\mathbf{MM^T}$:

$$\mathbf{M}(q,z)\mathbf{M}^{\mathbf{T}}(q,z)\tilde{\mathbf{E}}_{\mathbf{LO}}^{\lambda}(\vec{q}) = \lambda(z)\tilde{\mathbf{E}}_{\mathbf{LO}}^{\lambda}(\vec{q}). \tag{54}$$

One can easily see that the modes $\tilde{\mathbf{E}}_{\mathbf{LO}}(\vec{q})$ corresponding to different spatial frequencies are squeezed independently. For each spatial frequency, there are two eigenvalues,

$$\lambda_1 = (|\mu| + |\nu|)^2, \tag{55}$$

$$\lambda_2 = (|\mu| - |\nu|)^2, \tag{56}$$

with corresponding eigenvectors given by

$$\tilde{\mathbf{E}}_{\mathbf{LO}}^{\lambda_1}(\vec{q}) = \begin{bmatrix} \cos\varphi \\ \sin\varphi \end{bmatrix}, \tag{57}$$

$$\tilde{\mathbf{E}}_{\mathbf{LO}}^{\lambda_2}(\vec{q}) = \begin{bmatrix} \sin\varphi \\ -\cos\varphi \end{bmatrix}, \tag{58}$$

where

$$\varphi = \frac{\arg(\mu) + \arg(\nu)}{2}, \tag{59}$$

and the second eigenvector represents the electric field of the first shifted by $-\pi/2$. Note that the phase (59) is the eigenmode's phase at the output of the PSA. It is different from the optimum input phase

$$\theta = -\frac{\arg(\mu) - \arg(\nu)}{2} \tag{60}$$

that ensures maximum amplification. In other words, light entering the PSA with optimum input phase (60) will emerge from the PSA with output phase (59). Similarly, input light phase shifted by $-\pi/2$ from the phase (60) will emerge with $-\pi/2$ shift from phase (59). The eigenvalues of Equations (55) and (56) are related as $\lambda_1 = 1/\lambda_2$, which is a consequence of the symplectic transformation (16) leading to the condition $|\mu|^2 - |\nu^2| = 1$ for the Bogoliubov transformation (44).

From Equation (52), one can also obtain the normally-ordered correlator in the spatial ($\vec{\rho}$)-domain as

$$\begin{aligned}\mathbf{R}'(\vec{\rho}, \vec{\rho}\,', z) &= \int_0^\infty \mathbf{M}(q,z) J_0(q|\vec{\rho} - \vec{\rho}\,'|)\, q\, \mathrm{d}q/(2\pi) \\ &= \mathbf{R}'(|\vec{\rho} - \vec{\rho}\,'|, 0) + \mathbf{R}'_N(|\vec{\rho} - \vec{\rho}\,'|, z),\end{aligned} \tag{61}$$

where J_0 is the Bessel function and the initial correlator value is given by Equation (31). The four matrix elements of the correlator $\mathbf{R}'_N(|\vec{\rho} - \vec{\rho}\,'|, L)$ are plotted as functions of $\xi = |\vec{\rho} - \vec{\rho}\,'|$ in Figure 1(a) and as functions of $\vec{\xi} = \vec{\rho} - \vec{\rho}\,' = (\xi_x, \xi_y)$ in Figure 2(a) for a nonlinear crystal with parameter values similar to those in [3,7] and $\theta_p = -\pi/2$. The presence of the off-diagonal elements indicates that the quantum field

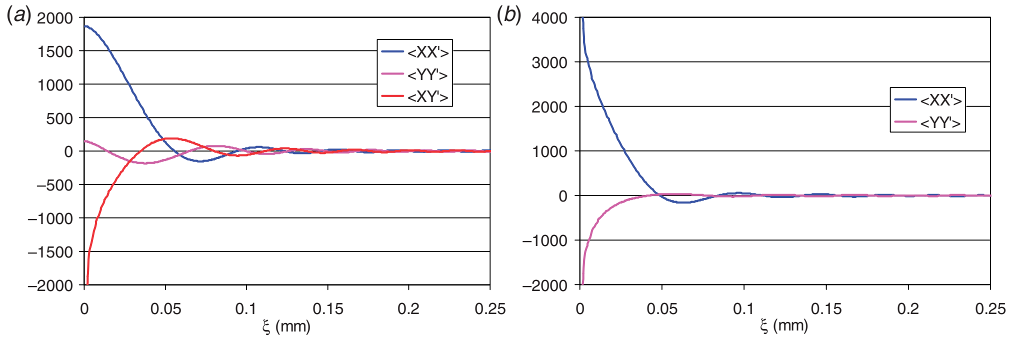

Figure 1. Diagonal and off-diagonal elements of the correlation matrix $\mathbf{R}'_N(\xi, L)$ of Equation (61) (where $\vec{\xi} = \vec{\rho} - \vec{\rho}'$ and $\xi = |\vec{\xi}|$) without (*a*) and with (*b*) a phase plate in the Fourier plane. Parameter values for the OPA are the same as those in [3,7]: crystal length $L = 5.21$ mm, $\Delta k = 0$, $\kappa L = 0.88$ [i.e. a phase-sensitive gain $(|\mu| + |\nu|)^2 = 5.8$ for $q = 0$], signal wavelength $\lambda_s = 1064$ nm, refractive index $n_s = 1.78$, and pump phase $\theta_p = -\pi/2$. (The color version of this figure is included in the online version of the journal.)

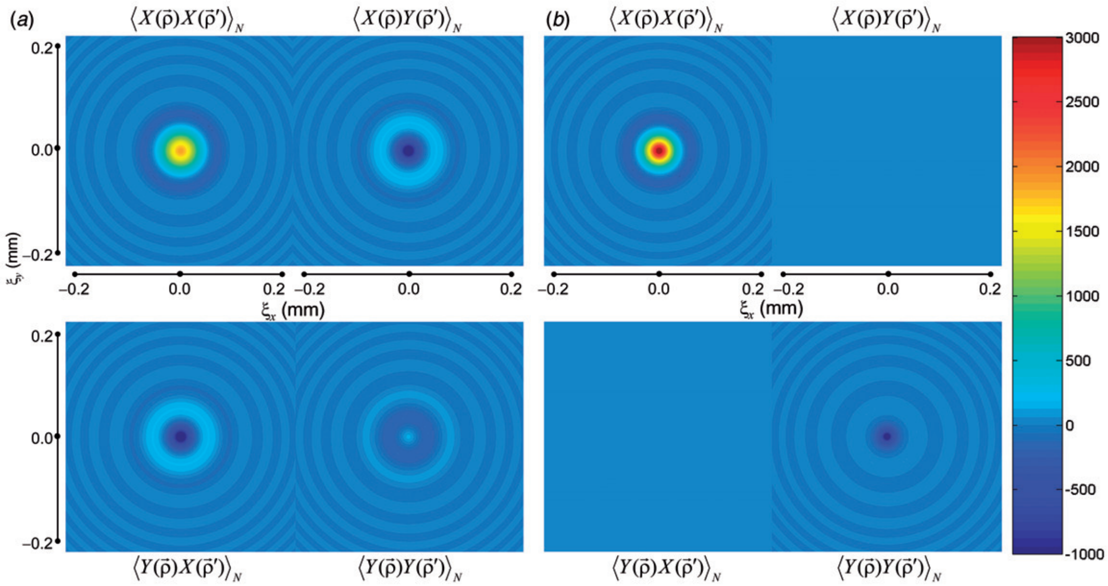

Figure 2. The diagonal and off-diagonal elements of the correlation matrix $\mathbf{R}'_N(\xi, L)$ of Figure 1 shown in the (ξ_x,ξ_y)-plane without (*a*) and with (*b*) a phase plate in the Fourier plane. (The color version of this figure is included in the online version of the journal.)

emerging from the OPA does not have a flat phase front. Such distortion can be corrected by inserting a Fourier-plane phase plate to rotate the phases of the spatial-frequency components of the output field by $-\phi(q)$ (for small parametric gains this can be approximated by a simple telescope that images the center of the crystal [7]). This transformation is equivalent to multiplication of Equation (51) by the matrix

$$\mathbf{S} = \begin{bmatrix} \cos\varphi & \sin\varphi \\ -\sin\varphi & \cos\varphi \end{bmatrix}, \tag{62}$$

which transforms the correlation matrix of Equation (52) into

$$\mathbf{S}\tilde{\mathbf{R}}'(\vec{q},\vec{q}',z)\mathbf{S}^{\mathbf{T}} = (2\pi)^2\delta(\vec{q}+\vec{q}')\begin{bmatrix} (|\mu|+|\nu|)^2 & 0 \\ 0 & (|\mu|-|\nu|)^2 \end{bmatrix}, \tag{63}$$

with the corresponding spatial-domain normally-ordered counterpart shown in Figures 1(*b*) and 2(*b*). The singularity at $\vec{\rho} = \vec{\rho}'$ is due to rectification of the sinc function in the spatial-frequency domain, which occurs when taking the absolute value of ν [7].

3.4. *Analytical solution 2: short crystal with inhomogeneous pump*

For sufficiently short crystals, the diffraction term in Equation (3) can be neglected, and the resulting equation takes the following form:

$$\frac{\partial E_s}{\partial z} = \frac{i\omega_s d_{\mathrm{eff}}}{n_s c} E_p E_i^* e^{i\Delta k z}, \tag{64}$$

or

$$\frac{\partial E_s}{\partial z} = i\kappa_s E_i^* e^{i\Delta k z}, \tag{65}$$

where $\kappa_s = \omega_s\ d_{\mathrm{eff}}\ E_p/(n_s\ c)$, in general, is a complex parameter that depends on the coordinate $\vec{\rho}$ (if the pump is inhomogeneous). One can then introduce the parameters μ and ν as

$$\begin{aligned}\mu(\vec{\rho}, z) &= \left(\cosh \gamma z - \frac{i\Delta k}{2\gamma}\sinh \gamma z\right) \times \exp\left(i\frac{\Delta k}{2}z\right),\\ \nu(\vec{\rho}, z) &= i\frac{\kappa_s}{\gamma}\sinh \gamma z\ \times \exp\left(i\frac{\Delta k}{2}z\right),\end{aligned} \tag{66}$$

where

$$\begin{aligned}\gamma(\vec{\rho}) &= \sqrt{\kappa^2(\vec{\rho}) - \Delta k^2/4},\\ \kappa^2 &= \kappa_s\kappa_i^* = \frac{\omega_s\omega_i d_{\mathrm{eff}}^2 I_p(\vec{\rho})}{2\varepsilon_0 n_s n_i n_p c^3},\end{aligned} \tag{67}$$

so that the solution takes the form of point-by-point (pixel-by-pixel) field amplification:

$$E_s(\vec{\rho}, z) = \mu(\vec{\rho}, z)E_s(\vec{\rho}, 0) + \nu(\vec{\rho}, z)E_i^*(\vec{\rho}, 0). \tag{68}$$

In the degenerate case, we have

$$\begin{aligned}G_x(\vec{\rho}, \vec{\rho}', z) &= [\mu(\vec{\rho}, z) + \nu(\vec{\rho}, z)]\ \delta(\vec{\rho} - \vec{\rho}'),\\ G_y(\vec{\rho}, \vec{\rho}', z) &= [\mu(\vec{\rho}, z) - \nu(\vec{\rho}, z)]\ \delta(\vec{\rho} - \vec{\rho}'),\end{aligned} \tag{69}$$

and

$$\mathbf{G}(\vec{\rho}, \vec{\rho}', z) = \mathbf{M}(\vec{\rho}, z) \times \delta(\vec{\rho} - \vec{\rho}'), \tag{70}$$

where

$$\mathbf{M}(\vec{\rho}, z) = \begin{bmatrix} \mathrm{Re}(\mu+\nu) & -\mathrm{Im}(\mu-\nu) \\ \mathrm{Im}(\mu+\nu) & \mathrm{Re}(\mu-\nu) \end{bmatrix}. \tag{71}$$

From Equations (70) and (71) we can see that the situation is very similar to the plane-wave pump case, but, instead of the spatial-frequency domain, the same input–output relations take place in the image domain. Namely,

$$\mathbf{E}(\vec{\rho}, z) = \mathbf{M}(\vec{\rho}, z)\mathbf{E}(\vec{\rho}, 0) \tag{72}$$

and

$$\begin{aligned}\mathbf{R}'(\vec{\rho}, \vec{\rho}', z) &= \delta(\vec{\rho} - \vec{\rho}') \times \mathbf{M}(\vec{\rho}, z)\mathbf{M}^{\mathbf{T}}(\vec{\rho}, z)\\ &= \delta(\vec{\rho} - \vec{\rho}')\begin{bmatrix} |\mu+\nu^*|^2 & 2\mathrm{Im}(\mu\nu) \\ 2\mathrm{Im}(\mu\nu) & |\mu-\nu^*|^2 \end{bmatrix},\end{aligned} \tag{73}$$

so that the independently-squeezed modes are the eigenvectors of the matrix $\mathbf{MM^T}$:

$$\mathbf{M}(\vec{\rho}, z)\mathbf{M}^{\mathbf{T}}(\vec{\rho}, z)\mathbf{E}_{\mathbf{LO}}^{\lambda}(\vec{\rho}) = \lambda(z)\mathbf{E}_{\mathbf{LO}}^{\lambda}(\vec{\rho}). \tag{74}$$

One can easily see that the modes $\mathbf{E}_{\mathbf{LO}}^{\lambda}(\vec{\rho})$ corresponding to different pixels of the image are squeezed independently. For each pixel, there are two eigenvalues,

$$\lambda_1 = (|\mu| + |\nu|)^2, \tag{75}$$

$$\lambda_2 = (|\mu| - |\nu|)^2, \tag{76}$$

with corresponding eigenvectors

$$\mathbf{E}_{\mathbf{LO}}^{\lambda_1}(\vec{\rho}) = \begin{bmatrix} \cos\varphi \\ \sin\varphi \end{bmatrix}, \tag{77}$$

$$\mathbf{E}_{\mathbf{LO}}^{\lambda_2}(\vec{\rho}) = \begin{bmatrix} \sin\varphi \\ -\cos\varphi \end{bmatrix}, \tag{78}$$

where

$$\varphi = \frac{\arg(\mu) + \arg(\nu)}{2}, \tag{79}$$

and the second eigenvector represents the electric field of the first shifted by $-\pi/2$. Similar to our discussion above for the plane-wave pump case, we note that the phase (79) is the eigenmode's phase at the output of the PSA. It is different from the optimum input phase

$$\theta = -\frac{\arg(\mu) - \arg(\nu)}{2} \tag{80}$$

that ensures maximum amplification. In other words, light entering the PSA with optimum input phase (80) will emerge from the PSA with output phase (79). Similarly, input light with phase shifted by $-\pi/2$ from the phase (80) will emerge with $-\pi/2$ shift from phase (79). The eigenvalues of Equations (75) and (76) are related as $\lambda_1 = 1/\lambda_2$, which is a consequence of the symplectic transformation (16) leading to the condition $|\mu|^2 - |\nu|^2 = 1$ for the Bogoliubov transformation (68).

4. Summary

We have presented a methodology for the complete quantum description of a traveling-wave phase-sensitive optical parametric amplifier (OPA) in terms of its normally-ordered quadrature correlators that are obtainable from the numerically or analytically solvable Green's function of the classical OPA propagation equation. This approach applies to the case of a pump beam with arbitrary spatial profile and enables determination of the independently-squeezed orthogonal eigenmodes of the OPA. This methodology serves as a basis for our study of the modes of the OPA with an elliptical Gaussian pump beam, which will be published elsewhere.

Acknowledgement

This work was supported by DARPA Quantum Sensors Program.

References

[1] Kolobov, M., Ed. *Quantum Imaging*; Springer Verlag: New York, 2007.
[2] Lantz, E.; Devaux, F. *IEEE J. Sel. Top. Quantum Electron.* **2008,** *14,* 635–647.
[3] Choi, S.-K., Vasilyev, M., Kumar, P. *Phys. Rev. Lett.* **1999**, *83*, 1938–1941; erratum: *Phys. Rev. Lett.* **200**, *84*, 1361–1361.
[4] Mosset, A.; Devaux, F.; Lantz, E. *Phys. Rev. Lett.* **2005,** *94,* 223603.
[5] Lopez, L.; Treps, N.; Chalopin, B.; Fabre, C.; Maître, A. *Phys. Rev. Lett.* **2008,** *100,* 013604.
[6] Gavrielides, A.; Peterson, P.; Cardimona, D. *J. Appl. Phys.* **1987,** *62,* 2640–2645.
[7] Vasilyev, M.; Stelmakh, N.; Kumar, P. *J. Mod. Opt.* **2009,** *56,* 2029–2033.
[8] Vasilyev, M.; Stelmakh, N.; Kumar, P. *Opt. Express* **2009,** *17,* 11415–11425.
[9] Schwob, C.; Cohadon, P.F.; Fabre, C.; Marte, M.A.M.; Ritsch, H.; Gatti, A.; Lugiato, L. *Appl. Phys. B* **1998,** *66,* 685–699.
[10] Kahraman, G.; Köprülü, K.G.; Aytür, O. *Phys. Rev. A* **1999,** *60,* 4122–4134.
[11] Patera, G.; Treps, N.; Fabre, C.; de Valcárcel, G.J. *Eur. Phys. J. D* **2009,** *56,* 123–140.
[12] Annamalai, M., Stelmakh, N., Vasilyev, M., Kumar, P. *Opt. Express*, to be submitted for publication, 2010.
[13] Yuen, H.P. *Phys. Rev. A* **1976,** *13,* 2226–2243.
[14] Yuen, H.P. *Nucl. Phys. B Proc. Suppl.* **1989,** *6,* 309.
[15] Shapiro, J.H.; Shakeel, A. *J. Opt. Soc. Am. B* **1997,** *14,* 232–249.
[16] Levandovsky, D.; Vasilyev, M.; Kumar, P. In *Quantum Communication, Computing, and Measurement 2:* Kumar, P., D'Ariano, G.M., Hirota, O., Eds.; Kluwer Academic/Plenum: New York, 2000; pp 469–474.
[17] Levandovsky, D. Quantum Noise Suppression Using Optical Fibers. Ph.D. Thesis, Northwestern University, 1999.
[18] McKinstrie, C.J. *Opt. Commun.* **2009,** *282,* 583–593.